FACCE-MACSUR

Paper on model responses to selected adverse weather conditions

Miroslav Trnka[1]*, Petr Hlavinka[2], Markéta Wimmerová[1], Eva Pohanková[1,2], Reimund Rötter[3], Jørgen E. Olesen[4], Kurt Christian Kersebaum[5] , Mikhail Semenov[6],

[1] Global Change Research Institute, Academy of sciences, Belidla 986/4, Brno, 60300, Czech Republic

[2] Mendel University in Brno, Zemedelska 1, Brno, 613 00, Czech Republic

[3] MTT Agrifood Research, 31600 Jokioinen, Finland

[4] Aarhus University, Frederiksborgvej 399, DK-4000, Århus, Denmark

[5] Leibniz Centre for Agricultural Landscape Research (ZALF) Eberswalder Straße 84 15374 Müncheberg, Germany

[6] Department of Computational and Systems Biology, Rothamsted Research, Harpenden AL5 2JQ, UK

*mirek_trnka@yahoo.com

Revision	Changes	Date
1.0	First Release	2017-05-30

Abstract/Executive summary

Based on the Trnka et al. (2015) study that indicated that heat and drought will be the most important stress factors for most of the European what area the further effort focused on these two extremes. The crop model HERMES has been tested for its ability to replicate correctly drought stress, heat stress and combination of both stresses. While data on the drought stress were available for both field and growth chambers, heat stress and its combination with heat stress was available only for the growth chambers. The modified version of the HERMES crop model was developed by Dr. Kersebaum and is being currently prepared for the journal paper publication.

Table of Contents

Introduction

Although inter-annual weather variability is well captured by crop models, extreme adverse weather conditions which are projected to increase across Europe (Trnka et al. 2014) are often not sufficiently considered in dynamic crop modeling. While in some cases processes such as extreme heat effects are still not fully understood, other extremes affect crop growth more physically than physiologically and reduce crop yield not only by real biomass losses, but additionally by impeding harvest processes (e.g. lodging). Additionally, weather situations adverse to perform optimal crop management such as sowing or harvest might affect crop production negatively. Additional to model improvements to capture some extremes physiologically, the implementation of agro-climatic indices and probabilistic approaches into crop models are required for a better assessment of climate change impact. Algorithms need to be developed and tested to consider adverse situations for cultivation such as sowing, harvest or fertilization to assess changes of management in climate change scenarios implied by these events of the first MACSUR phase to run models along whole crop rotations will be consequently continued.

Methods

At first we analysed the prevalance of the main adverse events. In this step the simulation of adverse weather events for wheat was performed for 379 European sites that represent the study domain (figure 1). In total, 36 European countries are represented by the study, covering the current European wheat-producing regions with the exception of Russia (figure 1*g*). Two GCMs from the CMIP5 ensemble were used with low, GISS-E2-R-CC (GISS), and high, HadGEM2-ES (HadGEM), climate sensitivity (electronic supplementary material, appendix figure S3). Two representative concentration pathway scenarios, RCP4.5 and RCP8.5, were considered in the construction of local-scale climate scenarios. Climate projections from GCMs were downscaled to the local-scale daily weather by the LARS-WG 6.0 weather generator using the ELPIS dataset of site-specific parameters across Europe. For each site and for each combination of GCMs and RCPs, we generated 300 years of daily site-specific weather, representing the baseline scenario corresponding to 1981–2010, and 300 years for the future climate scenario corresponding to 2081–2100. In each simulation, the first 50 years were used to initiate the calculation, and the remaining 250 years of data were retained for the subsequent analyses.

For each site, we used three types of cultivars according to the maturity date and two levels of photoperiod sensitivity as described by Trnka *et al.* 2014. The sowing, anthesis and maturity dates for the baseline conditions were estimated using AgriClim software, with the mean dates presented in the electronic supplementary material, appendix figure S4. It is assumed that cultivars represent winter wheat in all locations except those where temperature constrains vernalization. At these locations, we assumed that winter-sown spring wheat cultivars are used. For the entire study, autumn sowing dates were preferred to keep the sowing within the same season for all locations and facilitate comparisons among them. The sowing dates were determined automatically as the first day after the mean air temperature dropped below 13°C for more than five subsequent days with the soil moisture above one-third of its water-holding capacity. When calculating evapotranspiration, an adjustment for the atmospheric CO_2 concentration was made by reducing the reference evapotranspiration by a scaling factor. The value of the scaling factor for 2090 was estimated to be 0.94 for RCP4.5 and 0.88 for RCP8.5 of the baseline value. We used one soil profile for all of the sites, with homogeneous soil properties assumed throughout the top and subsoil layers to enable comparison among sites. The plant-available water at field capacity was assumed to be 270 mm in the entire profile (a depth of 1.3 m). We used a single free-draining soil with good water-holding properties and a relatively deep profile, allowing us to easily perform between-site comparisons of the climate signal.

To describe the major adverse conditions for wheat production, we used the following set of 11 indicators: indicators of frost damage, water logging, lodging, heat stress, drought stress and adverse conditions during sowing and harvest. To provide a measure of the potential productivity of a given site, we used the sum of the EfGr. We calculated the cumulative global radiation for days with a daily mean air temperature above 5°C, daily minimum air temperature above 0°C, no snow cover and actual-to-reference evapotranspiration ratio above 0.4. To define subregions and assign appropriate weights, Thiesen polygons (figure 1*g*) were used to assign areas represented by each station.
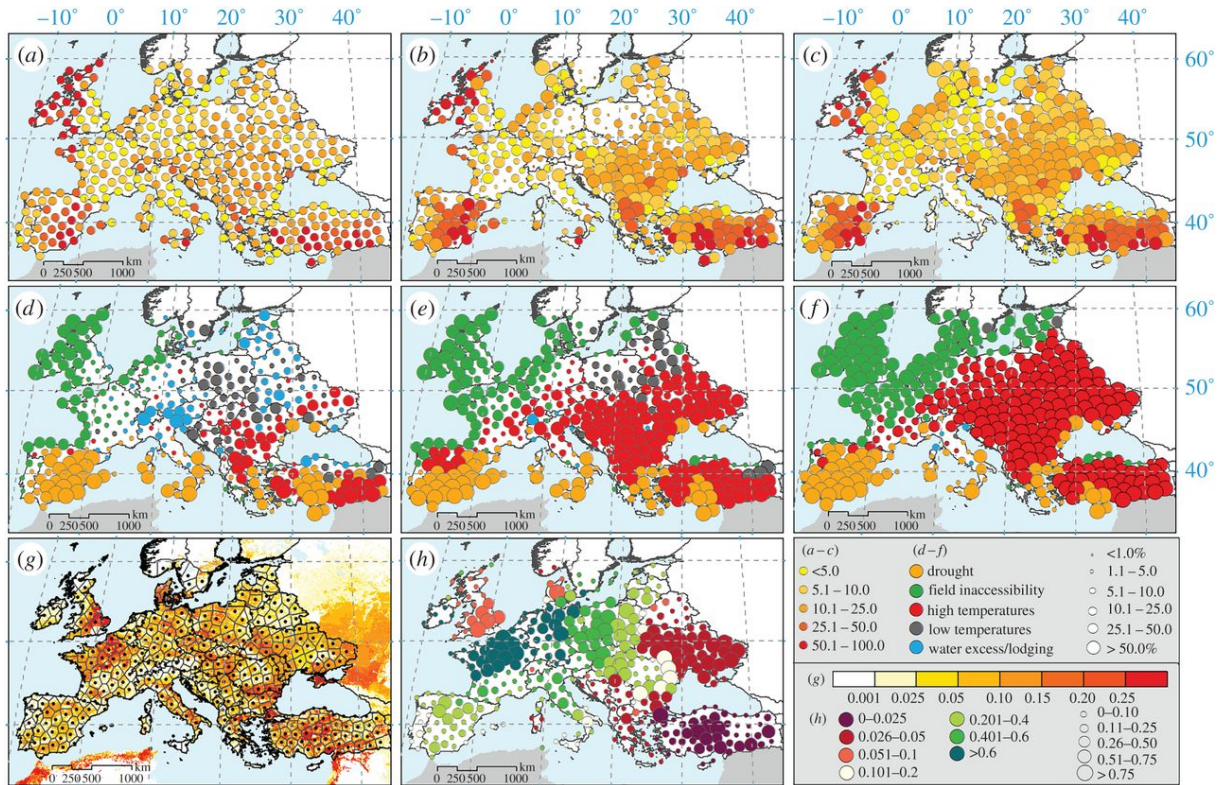
Fig. 1. Combined probability of a single adverse event over (a) the baseline, (b) GISS-RCP8.5 and (c) HadGEM-RCP8.5 scenarios with the size of the circle corresponding to the relative change compared to the baseline. (d) The dominant type of adverse event for the baseline, (e) for GISS-RCP8.5 and (f) for HadGEM-RCP8.5 with the size of the circle corresponding to the event frequency. (g) Proportion of wheat area in each grid (colour) in Europe based on Monfreda et al. [14] with the locations of 379 sites used in the study (thin lines are Thiesen polygons). (h) Colour-coding corresponds to the share of European wheat production per polygon, and the size of the circle corresponds to the proportion of the European wheat area represented by the polygon. Baseline (1981–2010) and climate scenarios (2081–2100).

In the next step the ability of HERMES model to emulate effects of drought and other stresses was tested. We used results of drought experiments conducted between 2012-2015 at the experimental site at Domanínek (Fig. 2). This selected model belongs among the widely used, easily accessible and well-documented crop growth simulation models (e.g. Palosuo et al. 2011). It is a process-oriented model for estimating development and growth of the field crops, soil water balance and the dynamics of nitrogen for arable land. The benefit of using HERMES is the ability to work with a relatively small amount of input data sets that are ordinarily available at the farm level and that take

into consideration plant growth, N-uptake, the process of net mineralization, the denitrification and transport of water and nitrate. The sub-model for crop growth was developed on the basis of the SUCROS model (van Keulen et al. 1982). The daily net dry matter production by photosynthesis, respiration, global radiation and temperature was simulated (Kersebaum et al. 2011). Crop growth was capped by water and nitrogen stress. Drought stress was indicated by the ratio of actual and potential transpiration. The dynamics of soil water were derived from a simple capacity approach. According to Kersebaum (2011), field capacity, wilting point and porosity may either be provided directly or applied from the stone content, texture and bulk density classes by German soil taxonomy.

The input data were divided into the following three parts: weather data, soil information and management data. Individual parameters entered into the model were obtained from soil and meteorological measurements including data about global solar radiation, air temperature (average, minimum and maximum), air humidity, wind speed, precipitation and tillage. Further, data of harvest, pre-crop and initial conditions were used to launch the model. These data were acquired from the Domanínek experimental station for the period 2013–2015. The average monthly air temperature and rainfall from sowing to harvesting are shown in Tab. II. The rainfall difference between the DRY and CONT plots was 93 mm (period from May to August).

a)

b)
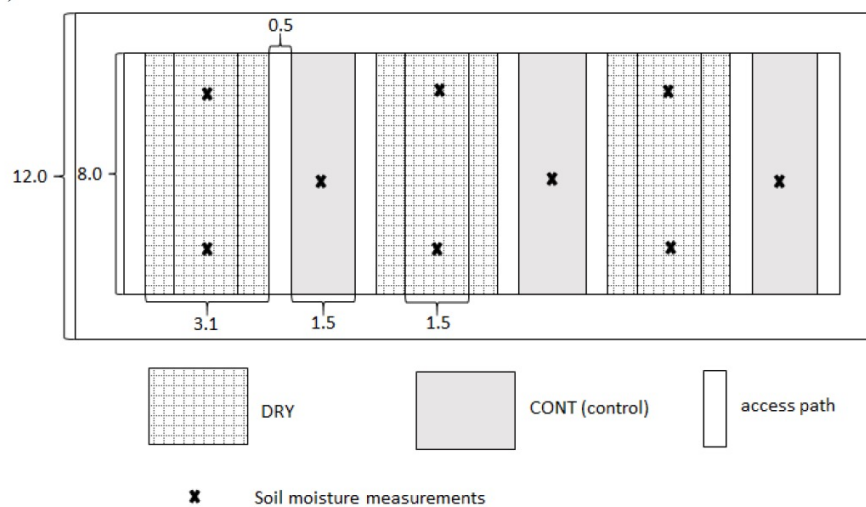
Fig. 2 (a) Illustrative photo. (b) Field trial map with the position of the rain-out shelters (DRY) and the TDR sensors for soil moisture measurements (figures are in meters).

Results

Under the present climate, the probability of a single adverse event is lower than 20% (i.e. once every 5 years) over the wheat-growing area that delivers 80% of the wheat in Europe. The core areas producing more than one-half of all European wheat are faced with some type of adverse event at least once every 10 years. Under both RCP4.5 and RCP8.5 scenarios, the probability of a single adverse event is predicted to increase considerably. Under the HadGEM-RCP8.5 climate scenario, by 2090 only 10% of European wheat production would be affected by a single adverse event less than once every 10 years, while one-half of the arable land area of Europe would be affected at least once every 2 years. There is a significant difference in the probabilities of a single adverse event between climate scenarios based on RCP4.5 and RCP8.5, with the latter showing a much greater increase in risk. There are also considerable differences in the probabilities of a single adverse event between climate scenarios based on the low-climate-sensitivity model (GISS) and the high-climate-sensitivity model (HadGEM). However, even a relatively 'favourable' climate scenario based on projections from GISS for RCP4.5 indicates a notably higher overall adverse event frequency. At present, therefore, most European wheat is grown in areas with a lower risk of adverse events relative to European arable land as a whole. Despite this, the exposure of the major wheat-producing areas to adverse events is predicted to increase more than twofold for the RCP8.5 and HadGEM model compared with a threefold increase over the entire available area of Europe's arable land. One of the critical conclusions was the illustrated at Fig. 1d-f showing that drought and heat are likely the dominating adverse events affecting wheat production (and in fact most of other crops as well).

The first step to evaluate the results correctly was to calibrate for crop phenology (emergence, tillering, heading, flowering and maturity) by approximating the conditions according to observed phenological phases (Fig. 3). The model was calibrated on the basis of measured and observed data from field experiments. Successive alteration temperature sums led to corresponding phenological phases. Therefore, observed values in each phenological phase for the CONT and DRY variants did not change. Fig. 3 shows both variants at the same level. The phenological phase of emergence occurred 13 days after sowing. Winter wheat began to form tiller after 62 days. The other phenological phases of heading, flowering and maturity occurred at 153, 164 and 218 days, respectively, in 2015. After calibration, the model showed almost the same results as measured values. Under the phenological phase of maturity, the model underestimated the DRY variant by 11 days.

a) Emergence and tillering

CONT_emergence   DRY_emergence
CONT_tillering   DRY_tillering

b) Heading, flowering and maturity

CONT_heading   DRY_heading
CONT_flowering   DRY_flowering
CONT_maturity   DRY_maturity
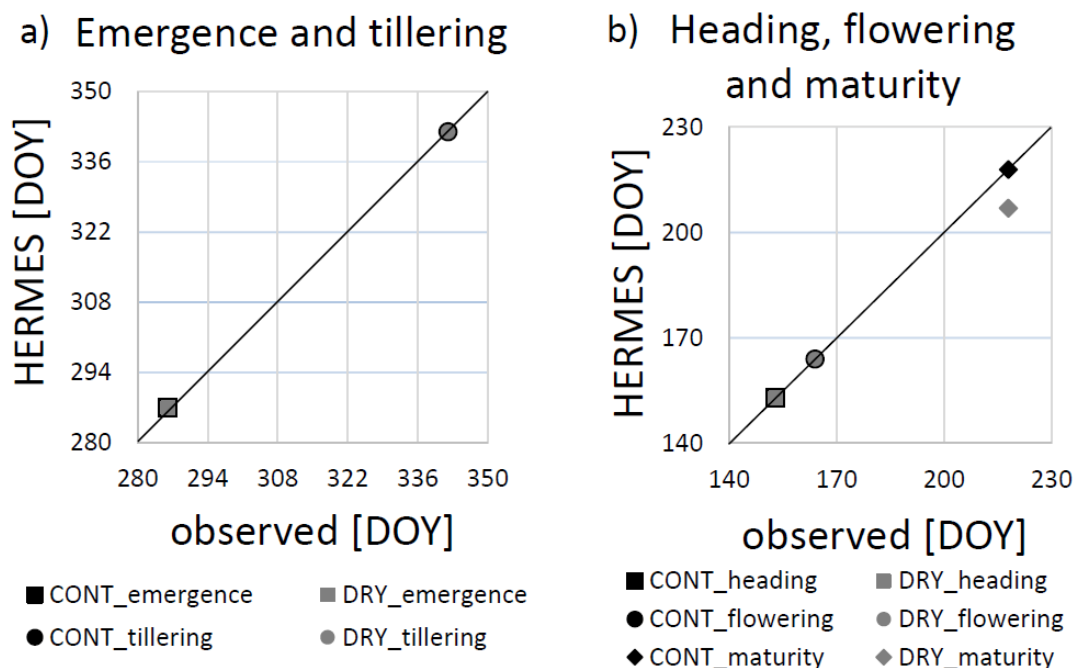
Fig. 3 Phenological phases observed and modeled. (a) From emergence to tillering and (b) from heading to maturity in days of the year (DOY).

Regarding leaf area development, the crop growth model overestimated that development (Fig. 4). Considering that 2015 was arid, the wheat was low and had sparse participation. Furthermore, it is necessary to take into account the fact that the HERMES model simulates only the leaf area, while measuring with SunScan covers a total above-ground area of plants. Therefore, the measurement points should be above simulated curves. It is necessary to recalibrate the model from ongoing measurements to obtain more precise results from the HERMES model. The results from further seasons will be used for this recalibration. In Palosuo et al. (2011), which compared models for winter wheat, the HERMES model led the average. In the current study, the HERMES crop growth model was able to evaluate the CONT option a little bit better than the DRY variant. However, the differences between the CONT and DRY variants were almost similar within the simulated and measured leaf area index. Conversely, the model captured the growth dynamics of the leaf area at similar levels as in Pohanková et al. (2013).

Evaluation of soil moisture using the TDR sensors was very satisfactory. Within the DRY variant, modeled results were evaluated as a nearly flat curve, confirming the roofs were waterproof (Fig. 5b). The CONT variant depicted changes in soil moisture under the influence of precipitation with good precision when compared with the curves of controls (Fig. 5a). Figs. 5a, 5b show the entire period from sowing to the end of August. The simulated curve also corresponded relatively and sufficiently to the shape of curve values measured by the TDR sensors. Overall, the HERMES model estimated soil moisture very accurately, e.g. comparable to Pohanková et al. (2013), which compared the results of two models (HERMES, DAISY) at the experimental station in Domanínek. Model credibility was validated based on crop model inter-comparison by Palosuo et al. (2011) and Rötter et al. (2012), where the HERMES crop growth model estimated soil water content with pinpoint accuracy. Real and simulated yields were compared in the next step (CONT vs. DRY).

The effect of the soil moisture shortage was reflected. For the CONT and DRY variants 2.65 and 0.94 t/ha grain yields, respectively, were measured. Using the rain-out shelters reduced real winter wheat yields by 1.7 t/ha. The model overestimated the yields in the uncovered variant (CONT) by an average of 0.15 t/ha and underestimated the yields in the rain-out shelters variant (DRY) by an average of 0.67 t/ha (Fig. 7).
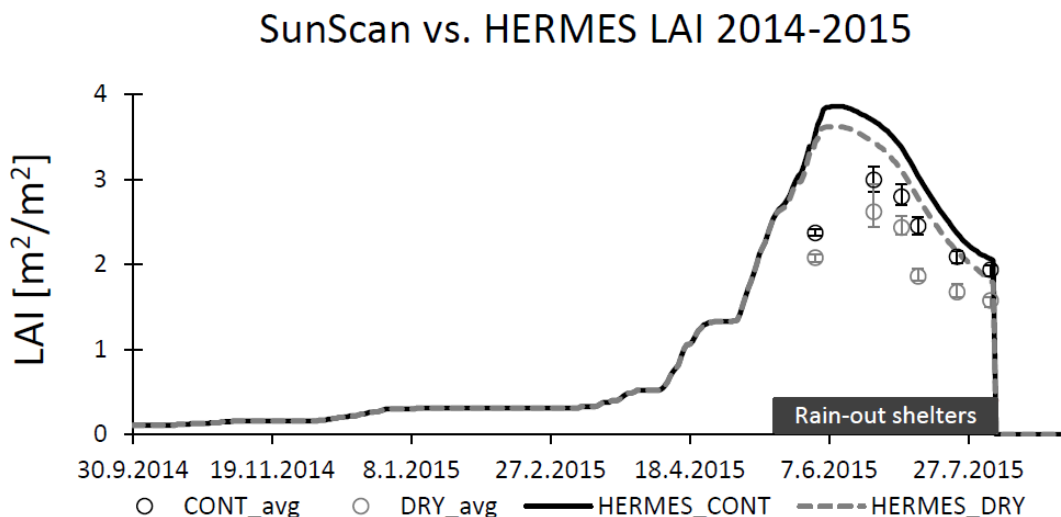
Fig. 4 SunScan measurements compared with simulated LAI. The average measured values are indicated with circles. The whiskers extend to the most extreme (minimum/maximum) measured values. A black box depict sheltered period (from 19th May to 6th August 2015).

a) Soil moisture outside the rain-out shelters

b) Soil moisture under the rain-out shelters
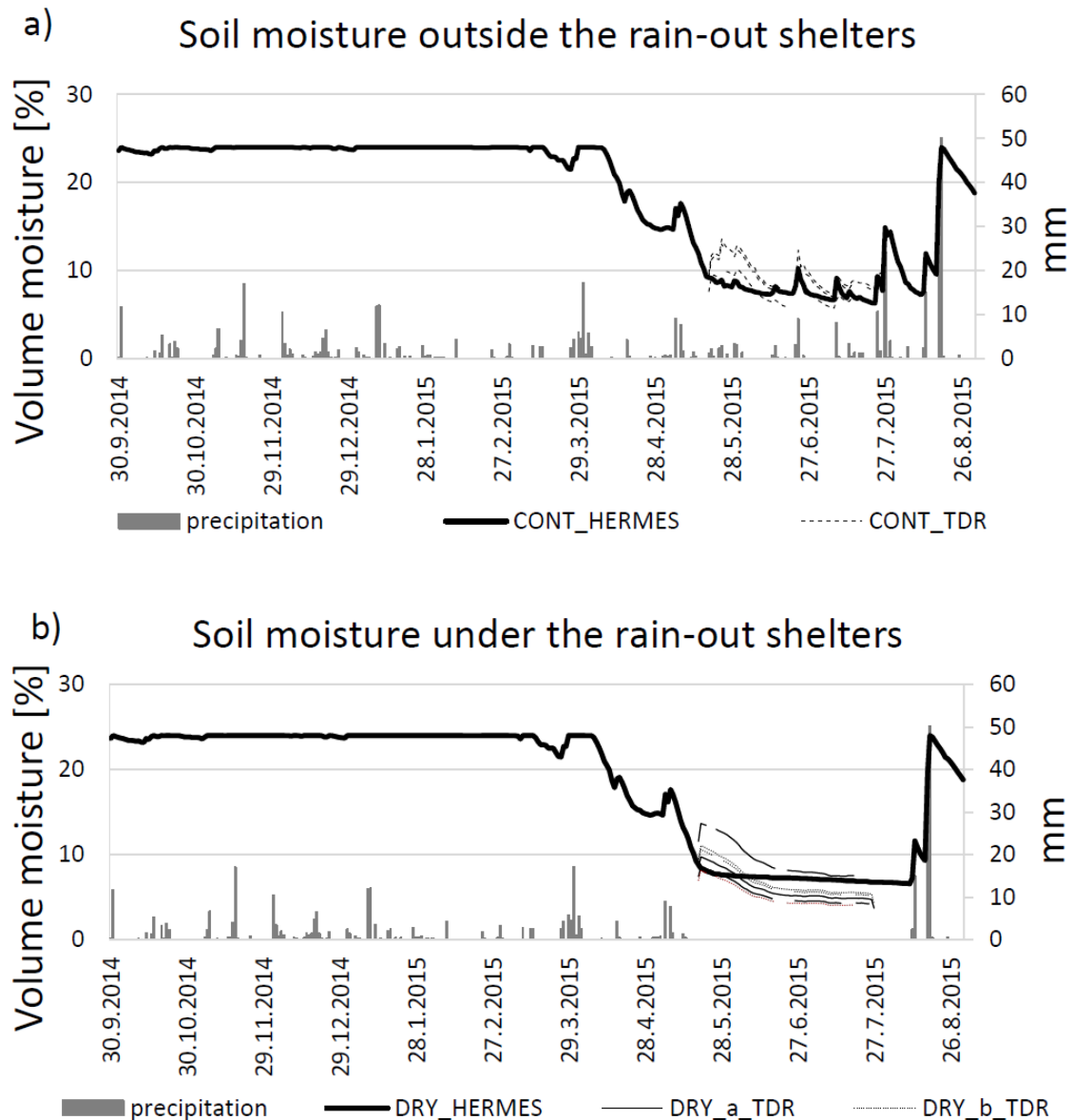
Fig. 5 Comparisons between the simulated and measured (under the rain-out shelters and outside) soil water content from 0.0 to 0.3 m. (a) Control (CONT) represents measurement outside the rain-out shelters for three repetitions. (b) DRY_a_TDR and DRY_b_TDR depict repetitions of the TDR sensors that were placed under one roof. Gray columns represent precipitation. The period depicted is from sowing to the end of August.

References

KERSEBAUM, K. C. 2011. Special Features of the Hermes Model and Additional Procedures for Parametrization, Calibration, Validation, and Applications. In: *Ahuja, L.R., Ma, L. editors, Methods of Introducing System Models into Agricultural Research*. Madison, Wisconsin, Adv.Agric. Syst. Model. 2. Madison: ASA, CSSA, SSSA, 65–94.

VAN KEULEN, H., PENNING DE VRIES, F. W. T. and DREES, E. M. 1982. A summary model for crop growth. In: P*enning de Vries, F. W. T., van Laar, H. H. editors, Simulation of Plant Growth and Crop Production.* Wageningen, The Netherlands: Pudoc, 87–97.

PALOSUO, T., KERSEBAUM, K. C., ANGULO, C. et al. 2011. Simulation of winter wheat yield and its variability in different climates of Europe: A comparison of eight crop growth models. *European Journal of Agronomy*, 35(3): 103–114.

POHANKOVÁ, E., TRNKA, M., HLAVINKA, P., et al. 2013. Calibration of the crop growth models for winter wheat. In: *Proceedings of International PhD Students Conference MendelNet 2013.* Brno, Czech Republic, 20 November, Brno: Mendel University in Brno, Faculty of Agronomy, 130–135 [Online]. Available at: https://mnet.mendelu.cz/mendelnet2013/articles/41_pohankova_759.pdf. [Accessed: 2016, July 11].

RÖTTER, R. P, PALOSUO, T., KERSEBAUM, K. C. et al. 2012. Simulation of spring barley yield in different climatic zones of Northern and Central Europe: A comparison of nine crop models. *Field Crop Research*, 133: 23–36.

TRNKA M, HLAVINKA P AND SEMENOV MA, Adaptation options for wheat in Europe will be limited by increased adverse weather events under climate change. *J R Soc Interfarce* **12**:1–7 (2015).